URSI GASS 2021, Rome, Italy, 28 August - 4 September 2021

Short Chorus Packets in Radiation Belts: Statistics and Role in Energetic Electron Acceleration

Xiao-Jia Zhang[(1)], Didier Mourenas[(2)(3)], Anton V. Artemyev[(1)], and Vassilis Angelopoulos[(1)]
(1) Department of Earth, Planetary, and Space Sciences, University of California, Los Angeles, California, USA
(2) CEA, DAM, DIF, Arpajon, France
(3) Laboratoire Matière en Conditions Extrêmes, Paris-Saclay University, CEA, Bruyères-le-Châtel, France

Abstract

Whistler-mode chorus waves contribute significantly to electron acceleration in Earth's radiation belts. It is unclear, however, whether the observed acceleration can be well described by quasi-linear theory alone, or if this acceleration is due to intense waves that require a nonlinear treatment. This paper reports on a comprehensive statistical analysis of 8 years of lower-band chorus wave packets measured by the Van Allen Probes and THEMIS spacecraft, performed to examine whether, when, and where these waves are above the theoretical threshold for nonlinear resonant wave-particle interaction. We find that $\sim 5-30\%$ of all chorus waves may interact nonlinearly with $\sim 30-300$ keV electrons. Such considerable occurrence rates of nonlinear interaction imply that the evolution of energetic electron fluxes should be dominated by nonlinear effects, rather than by quasi-linear diffusion as commonly assumed. However, we also find that only 15% of the wave power is carried by long packets considered in classical nonlinear models of wave-particle interaction, whereas 85% of the wave power comes from short packets with large frequency variations. We show that observed frequency fluctuations significantly reduce acceleration rates to realistic, moderate levels. Our results explain why global diffusive models of wave-particle interaction may statistically explain radiation belt dynamics, despite the fact that most observed wave amplitudes well exceed the maximum amplitudes for a safe application of the quasi-linear theory.

1 Introduction

The importance of resonant electron interactions with whistler-mode waves for radiation belt dynamics has spurred many observational and theoretical investigations in the past couple of decades. The background geomagnetic field inhomogeneity and the presence of multiple resonant interactions during a single electron bounce period along a field line often guarantees an effective randomization of electron motion [2] and, thus, justifies the applicability of the quasi-linear theory for modeling electron resonant scattering by sufficiently low amplitude waves. However, recent spacecraft observations [4] have revealed the existence of a statistically significant population of high-amplitude whistler-mode chorus waves that can potentially interact with electrons in the nonlinear regime (e.g., [7, 3, 6]) and lead to effects such as electron phase trapping and nonlinear scattering (sometimes called phase bunching) (e.g., see review by [12] and references therein). Although the effect of these nonlinear interactions on particle acceleration may be demonstrated for some short-duration events [1], the relative importance of nonlinear interactions, compared with quasi-linear scattering, for radiation belt dynamics is still poorly understood. In particular, quasi-linear diffusion models have been able to successfully reproduce the observed increase of relativistic electron fluxes over several days following large geomagnetic storms [14], casting doubt on the overall importance of nonlinear interactions for particle acceleration in the radiation belts.

To estimate the occurrence rate of chorus waves resonating with electrons nonlinearly, we built a dataset of lower-band chorus wave spectra (considering parallel propagating waves) measured by the Van Allen Probes and THEMIS [17]. Using these wave spectra, we determined the main characteristics of chorus waves, and calculated the inhomogeneity factor $|S|$ that determines the nature of wave-particle interaction [8, 10, 11]:

$$S = \frac{\left(1-N^{-2}\right)^{-1}\gamma}{kv_\perp\Omega_w}\left(1-v_R\frac{\partial k}{\partial\omega}\right)^2\frac{\partial\omega}{\partial t}+\frac{\left(1-N^{-2}\right)^{-1}}{2kv_\perp\Omega_w} \times \left(\frac{k\gamma v_\perp^2}{\Omega_{ce}}-\left(2+\left(1-N^{-2}\right)\frac{\Omega_{ce}-\gamma\omega}{\Omega_{ce}-\omega}\right)\right)\frac{\partial\Omega_{ce}}{\partial s}$$

where ω denotes wave frequency, Ω_{ce} the electron gyrofrequency, k the wave vector, $N=kc/\omega$ the wave refractive index, $v_\perp = c\sqrt{1-\gamma^{-2}}\sin\alpha$ the electron transverse velocity, γ and α the Lorentz factor and pitch angle of resonant electrons, $\Omega_w = eB_w/m_ec$ the wave amplitude, $v_R=(\omega-\Omega_{ce}/\gamma)/k$ the resonant velocity, and $\partial/\partial s$ the gradient along magnetic field lines. All parameters should be evaluated at the latitude satisfying the cyclotron resonance condition. For sufficiently large wave amplitudes, $|S|$ becomes less than one, meaning that such waves can interact with electrons in the nonlinear regime.

Figure 1 shows the percentage of lower-band chorus waves with $|S|<1$ as a function of electron energy and equatorial pitch angle, for two L-shell ranges: $4<L<6$ (in the outer radiation belt) and $6<L<10$ (in the nominal injection

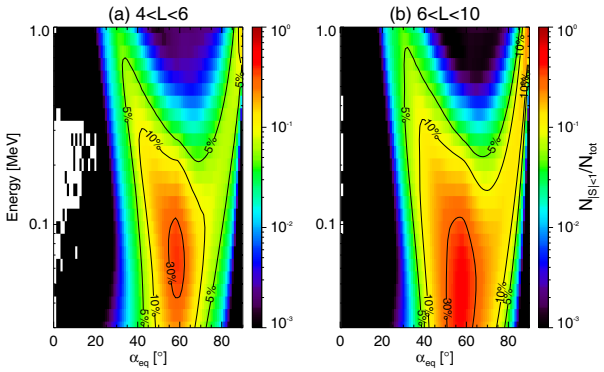

Figure 1. Maximum percentage of lower-band chorus waves likely to interact with electrons in the nonlinear regime for (a) 4<L<6 and (b) 6<L<10 [17].

region). The maximum percentage of lower-band chorus waves having sufficiently large amplitudes to reach $|S| < 1$ and interact nonlinearly with $\alpha_{eq} \sim 40-60^{\circ}$ electrons is higher than 30% below ~ 100 keV and remains higher than 10% below ~ 300 keV.

Figure 1 demonstrates considerable occurrence rates of nonlinear wave-particle interaction. Consequently, the observed evolution the outer radiation belt electron fluxes should mostly result from fast nonlinear effects (phase trapping and bunching), rather than from the much weaker and slower quasi-linear scattering that is still commonly assumed in many works. However, in many events with high amplitude chorus waves, quasi-linear diffusion models managed to reproduce relatively well the observed evolution of electron fluxes over long time scales of the order of days (e.g., see [14]). This suggests the possible presence of some additional parameters (in addition to wave amplitude and geomagnetic field inhomogeneity) that could significantly reduce the efficiency of nonlinear wave-particle interaction. This paper reviews recent results on the inner structure of intense chorus wave packets, demonstrating that majority of these waves propagate in the form of short packets of $< 10-20$ wave periods, with strong frequency variations, and that such strong wave amplitude and frequency variations can significantly reduce the efficiency of nonlinear wave-particle interaction, leaving more room for the quasi-linear theory.

2 Wave Packet Statistics

Using waveform measurements from the Van Allen Probes and THEMIS outside the plasmasphere, we selected all quasi-parallel (wave normal angle $< 25^{\circ}$) lower-band (in the 0.05-0.5Ω_{ce} frequency range, where Ω_{ce} is the equatorial electron gyrofrequency) chorus wave packets, bounded by two consecutive minima (< 50 pT) of the wave magnetic field amplitude (see wave packet examples in Figure 2). The measured frequencies $\omega_{obs}(t)$ inside each wave packet were then fitted as $\omega_{fit}(t) = (\partial\omega/\partial t)t + \text{constant}$, with $\partial\omega/\partial t$ being the frequency sweep rate. The wave

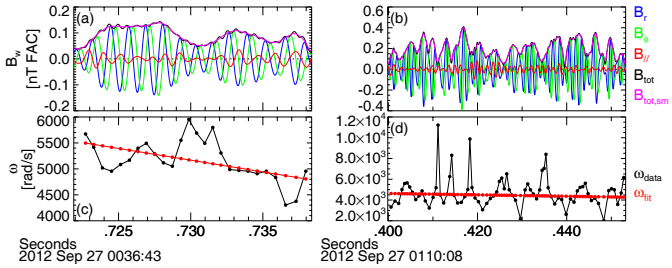

Figure 2. Two typical examples of short (left) and long (right) chorus wave packets. (a, b) Wave perpendicular (blue and green), parallel (red), and total magnetic field amplitude (original in black and smoothed in magenta); (c, d) observed (black) and fitted (red) wave frequency [17].

half-period is calculated as the interval between two consecutive zero crossings of the wave field. We defined here the packet length β as the number of wave periods during which the instantaneous wave amplitude remained within $[0.5B_{w_{peak}}, B_{w_{peak}}]$, without overlapping adjacent packets.

Figure 3(a) shows the distribution of separate chorus wave packets, as defined above, in the $(B_{w_{peak}}, \beta)$ space for the L-shell range of the outer radiation belt. The overwhelming majority of the observed chorus wave packets are rather short, with $\beta \leq 10$, representing $\sim 85\%$ of the total time-integrated chorus wave power. The distribution of wave-packet lengths clearly peaks around $\beta \sim 3$ over the whole domain 0.05 nT $< B_{w_{peak}} <$ 0.5 nT of maximum occurrences. However, the length of the most intense – but much more rare – wave packets can occasionally reach up to $\beta \sim 100$. Statistical results on the frequency variation inside such wave packets are shown in Figure 3(b,c): we focus on the observed rising frequency ($\partial\omega/\partial t > 0$) waves.

Figure 3(a) shows the distribution of frequency sweep rates $\partial f/\partial t$ (in kHz/s) inside lower-band chorus wave packets, as a function of wave packet length β and peak amplitude $B_{w,peak}$. The contours in Figure 3(a) show the occurrence rate of wave packets (see caption for levels). These contours indicate that most wave packets are short ($\beta < 30$) and low amplitude (< 0.2 nT), as previously noted [17]. This implies that most wave packets with $\beta < 10-20$ and low amplitudes have extremely high sweep rates, which is inconsistent with theory. Even for long wave packets with $\beta \sim 50-200$, in an intermediate range of amplitudes (0.25 nT $< B_{w,peak} <$ 0.6 nT), $\partial f/\partial t$ is nearly independent of $B_{w,peak}$, contrary to theoretical expectations. Our observations suggest that the frequency sweep rate of such short or intermediate-amplitude long wave packets may not only relate to the usual nonlinear evolution of the electron distribution (hole or step formation) on which the classical theory of wave generation is based [15, 11].

Figure 3(c) shows the event distribution of the normalized parameter $\beta(\partial\omega/\partial t)/\langle\omega\rangle^2$ as a function of packet length β (with $\langle\omega\rangle$ the average wave frequency within a packet). The parameter $\beta(\partial\omega/\partial t)/\langle\omega\rangle^2 = (df/\langle f\rangle)/2\pi$ is proportional

to the relative variation of the wave frequency ($df/\langle f\rangle$) over the wave packet duration $\beta/\langle f\rangle$ due to the measured sweep rate $\partial f/\partial t$. In Figure 3(c), $\beta(\partial\omega/\partial t)/\langle\omega\rangle^2$ most often decreases or remains constant as β increases. This indicates that wave packet length and sweep rate are anti-correlated. For long wave packets and/or small $\partial f/\partial t$, the mean relative frequency variation ($df/\langle f\rangle$) over wave packet duration increases linearly with β from low levels, which is indicative of a frequency sweep rate independent of packet length β. The variation of $\beta(\partial\omega/\partial t)/\langle\omega\rangle^2$ as a function of β, for a fixed sweep rate $\partial f/\partial t = 5$ kHz/s typical of nonlinear chorus wave growth theory, is plotted in Figure 3(c) for $\langle\omega\rangle/\Omega_{ce} = 0.4$ at $L = 5$ (lower black line), showing a good agreement between observations and theoretical expectations in the low $\partial\omega/\partial t$ and high β domains. For very long rising-frequency packets with $\beta > 100$, $\beta(\partial\omega/\partial t)/\langle\omega\rangle^2$ reaches an upper limit of $\simeq 0.12$, corresponding to a maximum frequency variation $df/\langle f\rangle < 0.75$ over packet duration. This is likely due to the limited frequency range of lower-band chorus waves. For rising tones starting from $\omega \geq 0.2\Omega_{ce}$, this upper limit indeed corresponds to the limit $\omega < 0.45\Omega_{ce}$ imposed by strong linear and nonlinear Landau damping near $0.5\Omega_{ce}$ [11].

In addition, Figure 3(c) reveals an intriguing characteristic of short ($\beta < 20$) wave packets. For most of them, $\beta(\partial\omega/\partial t)/\langle\omega\rangle^2$ decreases as $1/\beta$ with increasing packet length β (see upper black line). The frequency sweep rate of moderate-amplitude ($\simeq 0.08-0.2$ nT) short packets shown in Figure 2(b) seems too high relative to the classical sweep rate in the nonlinear theory of individual chorus wave growth [15, 11]. These inconsistencies with theory suggest that the observed strong amplitude modulation of short wave packets could simply result from superposition of at least two coherent waves with a frequency difference, $\Delta\omega_*$ – this frequency difference determining the packet duration $\beta/\langle f\rangle = 2\pi/\Delta\omega_* = 1/\Delta f_*$ [13]. An average total frequency variation over packet length of the order of the frequency difference could lead to a very high sweep rate, $\langle|\partial f/\partial t|_{ws}\rangle \approx \Delta f_*/(\beta/\langle f\rangle) \approx \Delta f_*^2 \propto 1/\beta^2$. This would potentially explain the observed variation of $\beta(\partial\omega/\partial t)/\langle\omega\rangle^2$ over $2 < \beta < 20$ in Figure 2(c), as well as the very high sweep rates in Figure 2(b).

3 Effects on Wave-Particle Resonant Interaction

Since we found that short wave packets are likely often formed by a superposition of waves [17, 18], it is important to examine the direct consequences of such wave superposition on nonlinear wave-particle interactions. Accordingly, we examined the simple case of an interaction between energetic electrons and a superposition of two coherent chorus wave packets, to understand the effect that the multiple resulting sub-packets may have in the electron acceleration process. Two packets with a frequency difference $\Delta\omega = 0$ (black and green curves in Figure 4) or $\Delta\omega/\omega \sim 1/5$ were

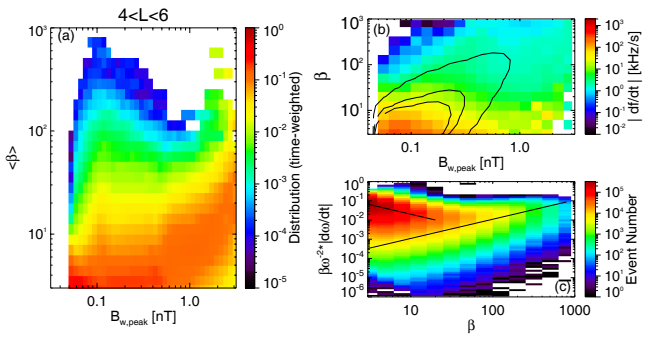

Figure 3. (a) Probability distribution of observed lower-band chorus wave packets in the $(B_{w_{peak}}, \beta)$ space for $L \in [4,6]$. Color coded is the temporal probability of a wave packet to fall into a specific peak amplitude ($B_{w_{peak}}$) and β bin. (b) Distribution of chorus frequency sweep rate, $\partial f/\partial t$ (in kHz/s), as a function of wave-packet length β (in number of wave periods $1/\langle f\rangle = 2\pi/\langle\omega\rangle$) and peak wave amplitude $B_{w,peak}$ of rising-frequency lower-band chorus wave packets. Solid black lines show contour levels of the distribution of packet occurrences (0.0005, 0.005, and 0.01 in downward direction). (c) Distribution of $\beta(\partial\omega/\partial t)/\langle\omega\rangle^2 = df/\langle f\rangle$ as a function of packet length (β). $\langle f\rangle$ and $\langle\omega\rangle$ denote the average wave frequency within the packet. Solid black lines show the typical variations in different parameter domains.

considered (blue and red curves in Figure 4), with constant or smoothly increasing frequency [16]. The distribution of energy changes ΔE obtained from test-particle simulations (for a single resonant interaction) for a realistic $\Delta\omega/\omega \sim 1/5$ corresponding to the presence of many sub-packets, has similar populations of accelerated trapped electrons and decelerated phase-bunched electrons, and a strongly reduced nonlinear acceleration compared to results for one long packet ($\Delta\omega = 0$). Realistic frequency/phase fluctuations make the ΔE distribution much more symmetric and limited to $|\Delta E| \leq 20$ keV, suppressing the strong trapping-induced acceleration by up to $\Delta E \sim 100$ keV (see Figure 4, red/blue curves versus black/green curves). Such a narrow and symmetric ΔE distribution should correspond to a more advective-like or diffusive-like long-term evolution of the electron distribution, as for independent short wave packets [9].

4 Conclusions

We have shown that most of the intense chorus waves that can potentially interact with electrons nonlinearly, propagate in the form of short wave packets with high frequency sweep rates. Strong frequency deviations from the linear sweep rate trend, larger than one tenth of the frequency over one wave period, are ubiquitous inside wave packets of all lengths [18]. All of these observed strong frequency variations may partly result from a local superposition of waves, leading to wave phase coherence loss between successive sub-packets [16]. A succession of independent, iso-

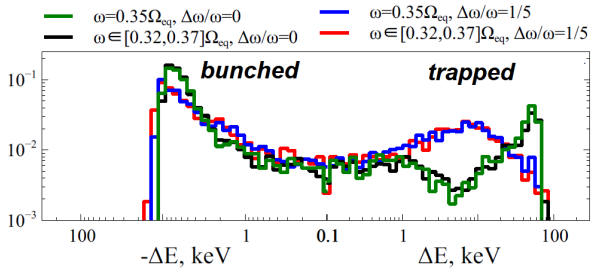

Figure 4. Results of particle scattering (for an initial electron energy of 500 keV and initial equatorial pitch angles of $\sim 40^\circ - 60^\circ$) by a superposition of two long wave packets with a total peak amplitude of $B_{w_{peak}} = 250$ pT and a frequency difference $\Delta\omega$. Distributions of positive and negative energy changes (ΔE) for a long wave-packet without amplitude modulations nor frequency jumps (for $\Delta\omega = 0$) and constant (green) or smoothly increasing mean frequency (black), and for a long wave-packet with frequency jumps and wave amplitude modulations (for $\Delta\omega/\omega = 1/5$), with constant (blue) or smoothly increasing mean frequency (red). [16]

lated short wave packets with $\beta < 5 - 10$, consisting of superposed waves of comparable and slowly varying amplitudes, could lead to electron energization and scattering that resemble more quasi-linear diffusion than nonlinear trapping acceleration and scattering [9, 16]. This could explain the success of quasi-linear diffusion codes in reproducing the observed multi-MeV electron energization during geomagnetic storms [14], despite the high amplitude of chorus wave packets [17].

5 Acknowledgements

X.J.Z. and A.V.A. acknowledge the support from NSF grants 2021749, 2026375 and NASA grant 80NSSC20K1578.

References

[1] O. V. Agapitov, et al. Nonlinear local parallel acceleration of electrons through Landau trapping by oblique whistler mode waves in the outer radiation belt. *Geophys. Res. Lett.*, 42:10, 2015.

[2] J. M. Albert. Diffusion by one wave and by many waves. *J. Geophys. Res.*, 115:0, 2010.

[3] J. Bortnik, R. M. Thorne, and U. S. Inan. Nonlinear interaction of energetic electrons with large amplitude chorus. *Geophys. Res. Lett.*, 35:21102, Nov. 2008.

[4] C. Cattell, et al. Discovery of very large amplitude whistler-mode waves in Earth's radiation belts. *Geophys. Res. Lett.*, 35:1105, Jan. 2008.

[5] C. M. Cully, et al. Observational evidence of the generation mechanism for rising-tone chorus. *Geophys. Res. Lett.*, 38:1106, Jan. 2011.

[6] A. G. Demekhov, et al. Efficiency of electron acceleration in the Earth's magnetosphere by whistler mode waves. *Geomagnetism and Aeronomy*, 49:24–29, Feb. 2009.

[7] N. Furuya, Y. Omura, and D. Summers. Relativistic turning acceleration of radiation belt electrons by whistler mode chorus. *J. Geophys. Res.*, 113:4224, Apr. 2008.

[8] V. I. Karpman. Nonlinear Effects in the ELF Waves Propagating along the Magnetic Field in the Magnetosphere. *Space Sci. Rev.*, 16:361–388, Sept. 1974.

[9] D. Mourenas, et al. Electron Nonlinear Resonant Interaction With Short and Intense Parallel Chorus Wave Packets. *J. Geophys. Res.*, 123:4979–4999, June 2018.

[10] D. Nunn. self-consistent theory of triggered VLF emissions. *Planatary Space Science*, 22:349, Mar. 1974.

[11] Y. Omura, Y. Katoh, and D. Summers. Theory and simulation of the generation of whistler-mode chorus. *J. Geophys. Res.*, 113:4223, Apr. 2008.

[12] D. R. Shklyar and H. Matsumoto. Oblique Whistler-Mode Waves in the Inhomogeneous Magnetospheric Plasma: Resonant Interactions with Energetic Charged Particles. *Surveys in Geophysics*, 30:55–104, Apr. 2009.

[13] X. Tao, et al. The importance of amplitude modulation in nonlinear interactions between electrons and large amplitude whistler waves. *Journal of Atmospheric and Solar-Terrestrial Physics*, 99:67–72, July 2013.

[14] R. M. Thorne, et al. Rapid local acceleration of relativistic radiation-belt electrons by magnetospheric chorus. *Nature*, 504:411–414, Dec. 2013.

[15] V. Y. Trakhtengerts, et al. Interpretation of Cluster data on chorus emissions using the backward wave oscillator model. *Physics of Plasmas*, 11:1345–1351, Apr. 2004.

[16] X. J. Zhang, et al. Phase Decoherence Within Intense Chorus Wave Packets Constrains the Efficiency of Nonlinear Resonant Electron Acceleration. *Geophys. Res. Lett.*, 47(20):e89807, Oct. 2020.

[17] X. J. Zhang, et al. Nonlinear Electron Interaction With Intense Chorus Waves: Statistics of Occurrence Rates. *Geophys. Res. Lett.*, 46(13):7182–7190, July 2019.

[18] X. J. Zhang, et al. Rapid Frequency Variations Within Intense Chorus Wave Packets. *Geophys. Res. Lett.*, 47(15):e88853, Aug. 2020.